Eur. Phys. J. D **29**, 235–245 (2004)
DOI: 10.1140/epjd/e2004-00051-1

THE EUROPEAN PHYSICAL JOURNAL D

Theoretical and experimental CARS rotational distributions of $H_2(X^1\Sigma_g^+)$ in a radio-frequency capacitive discharge plasma

V.A. Shakhatov[1], O. De Pascale[2], and M. Capitelli[2,3,a]

[1] Centro Laser s.r.l., S.P. per Casamassima, km 3, 70010 Valenzano (BA), Italy
[2] Istituto di Metodologie Inorganiche e dei Plasmi (CNR IMIP), c/o Dept. of Chemistry, Via Orabona 4, 70126 Bari, Italy
[3] Department of Chemistry, University of Bari, Via Orabona 4, 70126 Bari, Italy

Received 9 September 2003
Published online 15 April 2004 –

Abstract. Multiplex coherent anti-Stokes Raman scattering (CARS) spectroscopy is used for thermometry in H_2 radio-frequency capacitive discharge plasma at low gas temperature of 300−400 K, pressure of 0.4−4 Torr and power of 100 W. Results of the investigation of population densities of rotational levels in the ground electronic state of the hydrogen molecule and measurements of rotational temperature by multiplex H_2 CARS spectroscopy in H_2 radio-frequency capacitive discharge plasma are reported. Computational codes have been realized to determine the rotational and vibrational temperature and to analyze H_2 CARS spectrum for equilibrium and non-equilibrium conditions. To ensure the reliability of the rotational temperature measurements, we also apply method of scanning narrow-band CARS spectroscopy in our investigations.

PACS. 52.70.-m Plasma diagnostic techniques and instrumentation – 52.50.Dg Plasma sources – 42.62.Fi Laser spectroscopy

1 Introduction

R.F. capacitive discharge plasmas in molecular hydrogen at low pressure and gas temperature is a subject of intensive experimental and theoretical study as a consequence of their wide applications in technological processes [1,2].

It is well-known [3] that in such media temperatures corresponding to different degrees of freedom of the hydrogen molecule can differ considerably. The knowledge of the gas temperature in nonequilibrium conditions represents significant interest for plasma chemistry and study of plasma interaction with a surface, since rate constants of gas phase and heterogeneous reactions strongly depend on the gas temperature. For optimization of the technological processes it is urgent to develop diagnostic techniques for fast monitoring of gas temperature in such media.

Methods for gas temperature monitoring include pyrometry, thermocouple and spectral methods, interferometry [4] and laser spectroscopy techniques [5]. Time-resolved optical emission spectroscopy [6,7] and laser-induced fluorescence spectroscopy [8] are becoming increasingly popular for such measurements.

Moreover, vibrational-rotational distributions in the ground state of homonuclear molecules in discharges allow determining gas temperature. The rotational temperature deduced by measuring the relative intensities of the Q-branches of the homonuclear molecules within a particular vibrational manifold matches in fact the gas one due to the high rate constants of rotational-translational relaxation [2,3]. The study of the distributions can be carried out most effectively by methods of laser Raman-scattering spectroscopy, particularly by Coherent Anti-Stokes Raman Scattering (CARS) technique [9–11]. The CARS technique has a number of advantages, which greatly extend the possibilities of plasma diagnostics: the high spatial-temporal resolution ($100 \times 100 \times 1000$ μm, 10 ns) and the high spectral brilliance of the anti-Stokes signal, with a divergence close to that of the laser beam, make it possible to study objects and media with low densities down to 10^{14} cm^{-3}.

As far as concerns the studies on homonuclear diatomic molecules in various types of discharge [12–34], many papers [12–22] were devoted to the systematic study of the rotational and vibrational distributions of molecular nitrogen, definition of rate constants for VV (Vibration Vibration) energy exchange rates in nitrogen glow and pulsed discharges. These investigations have shown that the vibrational temperature can be higher than the rotational one. Under these conditions, the vibrational distribution strongly deviates from Boltzmann law, while the

[a] e-mail: m.capitelli@area.ba.cnr.it

rotational temperature is practically equal to the gas temperature.

The first use of CARS spectroscopy for the investigation of the rotational and vibrational distributions of molecular deuterium in a glow discharge was reported by Nibler et al. [23]. From these experiments, they estimated a vibrational temperature of about 1050 K with a rotational temperature of about 400 K. Soon after, Shirley et al. [24] reported measurements of vibrational excitation of molecular deuterium and hydrogen by spontaneous Raman scattering technique in a low pressure dc glow discharge. It was found that the vibrational temperature can reach values up to 1900. H_2-CARS technique has been successfully applied for gas temperature measurements in the reactive zone of a plasma arc test reactor for hydrocarbon synthesis [25], in hot-filament chemical-vapor deposition of diamond [26,27], in a microwave assisted diamond CVD plasma [28], in stagnation-flow diamond-forming flames [29], during the deposition of silicon carbide from methyltrichlorosilane [30] and in magnetic multiscusp H_2 and D_2 discharges [31]. It should be noted that the paper [26] is the only that, to our knowledge, has investigated the rotational distribution in H_2 r.f. inductive discharge plasma (at pressure of 5 Torr and power of 100−300 W). Measured values of the rotational temperature fall in the range between 300 and 400 K. Using CARS, Ochkin and co-workers [32,33] have measured the rotational populations of $H_2(X^1\Sigma_g^+)$ molecules in a low pressure (0.5−5 Torr) hydrogen discharge plasma cooled by liquid nitrogen. It has been observed that the rotational distribution deviates from the Boltzmann law for rotational levels with $J = 0-3$. An analogous result but for high rotational levels $J > 4$ was reported by Pealat et al. [31] and Lefebvre et al. [34] in magnetic multipolar-confined H_2 discharge. The behaviour of rotational distribution of hydrogen seems very different from nitrogen ones. A critical review of the experimental results reported in reference [35] shows that measurement of gas temperature in various types of discharges in molecular hydrogen is not trivial. A careful approach is necessary for an estimation of gas temperature. Therefore, carrying out a study with the purpose of new data acquisition or development of new techniques for gas temperature measurement in a hydrogen discharges are potentially interesting.

Traditionally, CARS spectra are recorded by the methods of scanning narrow-band [12–16,18–20,22–24,26,27, 30–34] and multiplex [25,28,29] CARS spectroscopy. A considerable time is needed to record spectra through scanning narrow-band, so that its use is limited to those cases when the investigated parameters do not change during the measurements. In the multiplex CARS spectroscopy method, involving the use of an optical multichannel analyzer, a considerable part of the CARS spectrum is recorded in a single laser shot thus reducing gas temperature evaluation times and, as a consequence, this method is more preferable for fast monitoring of gas temperature.

In the present study, the application of multiplex coherent anti-Stokes Raman scattering (CARS) spectroscopy is shown for thermometry in H_2 radio-frequency capacitive discharge plasma at low gas temperature of 300−400 K, pressure of 0.4−4 Torr and power of 100 W. Similarly to the results reported in reference [6], we do not expect that gas temperature exhibits time dependence on a time scale of r.f. period (about 37 ns). An investigation of population densities of the rotational levels $J = 0-3$ in the ground electronic state $X^1\Sigma_g^+$ of the hydrogen molecule and measurements of the rotational temperature by multiplex H_2 CARS spectroscopy in the r.f. capacitive discharge plasma are reported for the first time. Computational codes have been set-up to determine the rotational and vibrational temperatures and to analyze H_2 CARS spectrum under non-equilibrium conditions. To ensure the reliability of the rotational temperature measurements, we also apply the method of scanning narrow-band CARS spectroscopy in our investigations.

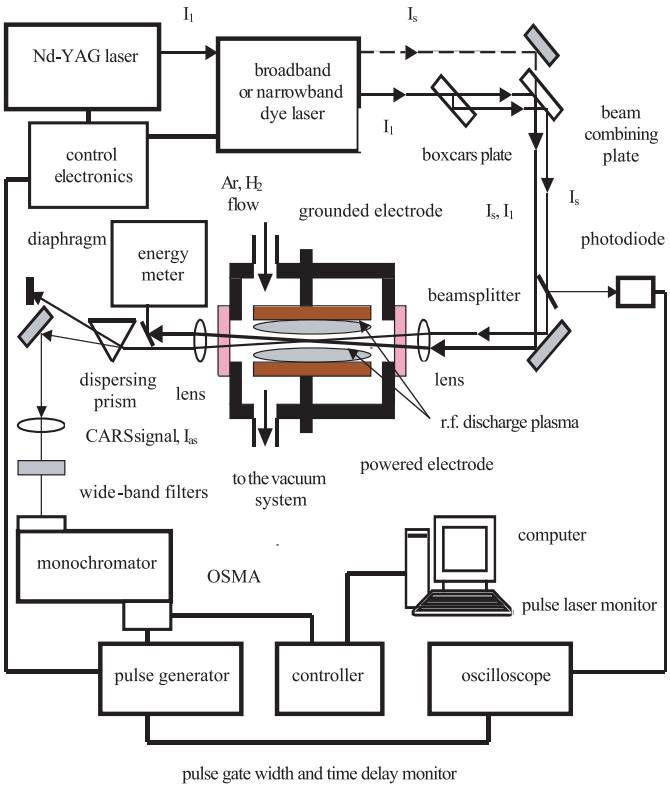

Fig. 1. Schematic diagram of the experimental set-up.

2 Experimental set-up

A schematic diagram of the experimental set-up is presented in Figure 1. It consists of the CARS system with optics to recombine and focus the pump laser beams for generating the CARS spectrum, a r.f. discharge reactor, a system for gas feeding and pumping out, and a pressure controlling system.

The r.f. discharge reactor is a typical stainless steel vacuum chamber of cylindrical geometry. It is equipped with

ports for the pump laser beams, gas pumping out and feeding and pressure gauging. The r.f. discharge geometry is a simple parallel plate design. The diameter of the parallel-plate electrodes is 10 cm with 2.0 cm inter-electrode distance, r.f. power typically 100 W at 27 MHz applied to the lower electrode (powered electrode) through an impedance-matching network. The upper electrode serves as grounded electrode. For most of the experiments, temperature of the upper-grounded electrode is floating and estimated close to room temperature. In some experiments, the upper electrode was heated and its temperature was controlled by a thermocouple.

The vacuum chamber is pumped up to 10^{-6} Torr by Balzers rotary and turbo-molecular pumps. Pressure is measured by Balzers total pressure gauge controller. Argon, at pressure 750 Torr, is used to record non-resonant CARS signal. The measurements of the rotational temperature are carried out under non-excited hydrogen flow or under hydrogen r.f. discharge plasma. The molecular hydrogen is produced by a generator (H_2 FLO 300-220 hydrogen generator). The total gas pressure is varied from 0.4 to 4 Torr. The gas flow and pressure into the chamber are regulated by gas dosing valve.

The CARS system allows realizing acquisition of spectra by the methods of scanning narrow-band or multiplex CARS spectroscopy. The CARS system includes also an automatic system for data acquisition and processing. Its laser system consists of an Nd–YAG laser with frequency doubling, and a narrow-band dye laser or a broadband dye laser depending on the method of acquisition of CARS spectra.

The Nd–YAG laser is formed of an oscillator, a parallel amplifier stage and second harmonic generation, with the pulse rate varying between 1 and 10 Hz, pulse width 25 ns, line-width 0.5 cm^{-1}, output energy as high as 100 mJ at 532 nm, where about 30% of the energy is used to pump the dye laser, while the remaining part is sent to the CARS combining optics.

The broadband dye laser is based on a very simple design, using an oscillator and an amplifier stage in a longitudinal pumping scheme, the bandwidth is approximately 600−615 cm^{-1}.

The narrowband dye laser contains an oscillator in combination with two amplifier stages. The oscillator consists of a 600 lines/mm grating used from the 3rd to the 8th order and an achromatic prism beam expander for narrowing the line-width and a dye cell. The grating is tilted by a high precision sine drive mechanism controlled by computer. Transversal pumping of the active medium of the oscillator and the amplifier with one-dimensional focusing of the pump beam by cylindrical lenses is applied. The line-width of the output beam is 0.8 cm^{-1}. The spectral resolution of the scanning narrow-band CARS spectrometer is estimated about 1 cm^{-1}.

To excite and observe rotational structure of the Q-branches of vibrational-rotational transitions $v = 0 \rightarrow v = 1$ and $v = 1 \rightarrow v = 2$ (v is the vibrational quantum number) in the electronic ground state of the hydrogen molecule, a mixture of the DCM and LDS 698 are adjusted to reach maximum efficiency at 680 nm. CARS spectrum covers the interval approximately between 3600 and 4325 cm^{-1}. An output energy of dye lasers is typically 1.0 mJ. The laser energy fluctuations of the dye and ND–YAG lasers are controlled during the experiments by an energy meter.

The CARS signal intensity is generated at high conversion efficiency under optimum phase matching conditions [9–11]. Both collinear and planar BOXCARS arrangements are employed in the experiments (see Fig. 1). The spatial resolution is defined by the CARS probe volume, i.e. the volume where the CARS signal is generated. Its size, in the crossbeam direction, was estimated to be the diameter of an aperture burned by the laser radiation in a thin aluminum foil, located in the focusing area of the primary laser radiation. In both the geometrical mixing scheme of the pump laser beams, the diameter of the CARS probe volume was approximately equal and was about 150−200 μm. The length of the CARS probe volume, in the beam direction, was appreciably different. In the collinear beam arrangement, for a Gaussian distribution of the radiation intensity of the pump lasers I_1 and I_s, 75% of the energy of the CARS signal I_{as} is generated in a focal region equal to a cylinder of diameter $D = 4\lambda(f/\pi)d$ and length $S = 3\pi D^2/\lambda$ [10], where d is the diameter of the laser beams in the plane of the lens, f is the focal length of the lens focusing the laser beams into the r.f. discharge chamber, and the value of S approximately estimates the spatial resolution in the direction of beam propagation. In our case $d = 0.7$ cm and $f = 25$ cm, hence $S = 10$ mm. The spatial resolution, in the beam direction, for the planar BOXCARS arrangement was better than in collinear beam arrangement, the length S was about 2 mm.

The useful CARS signal is separated from both the background radiation of the lasers and plasma by means of a dispersing prism and wide-band filters. To detect intensity distribution of H_2 CARS spectra, a high-resolution monochromator (HR640, Instruments S.A., division Jobin Yvon) equipped with a holographic grating 2400 gr/mm and an intensified optical simultaneous multichannel analyzer (OSMA) placed at the exit slit, is used.

During the experiments, the Nd–YAG laser control electronics triggers a pulse generator, which provides gating of the OSMA. The pulse generator is connected to the control electronics, a detector head and a controller for data acquisition accomplish the detection of CARS spectrum by OSMA. To control Nd–YAG laser timing jitter, a portion of the laser beam is split off by a glass wedge and detected by a fast photodiode. An oscilloscope is used to monitor laser pulse, gate width and time delay after laser irradiation. A gate width of 1.2 μs is used to maximize CARS line intensity. To optimize signal-to-noise ratio, monitoring of CARS signals is carried out in accumulation mode. Accumulation number is varied up to 100.

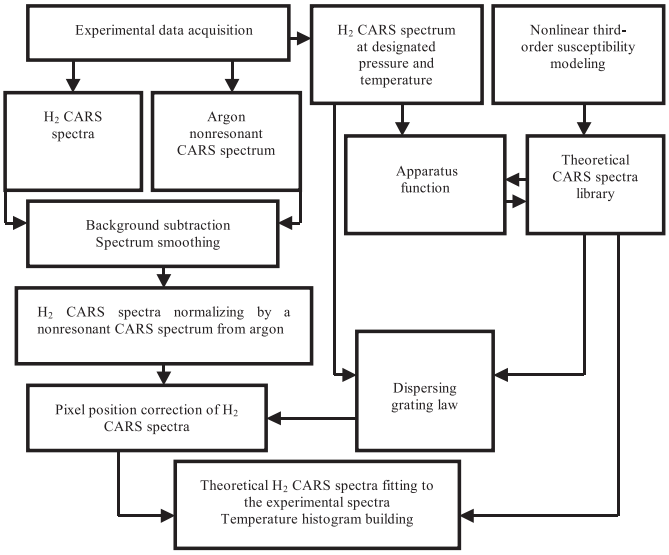

Fig. 2. Schematic diagram of the experimental data acquisition and processing.

3 Experimental data processing

The rotational temperature and distribution are deduced by two approaches. By the first approach, when we use the multiplex CARS spectroscopy method, the rotational temperature is evaluated by comparison of the experimental CARS spectrum with that predicted by theory [28,29]. Computational codes have been developed to determine the rotational and vibrational temperatures and to analyze H_2 CARS spectrum in nonequilibrium conditions, in the r.f. discharge plasma. By the second approach, when we apply the scanning narrow-band CARS spectroscopy method, the rotational temperature and distribution are deduced from measurements of rotational line amplitudes in the fundamental vibrational transition $v = 0{-}v = 1$ [12–16,18–20,22–24,26,27,30–34].

Figure 2 shows a schematic block diagram of experimental data processing, which we implemented to evaluate the rotational temperature and distribution by the first approach. In order to determine the average temperature with its standard deviation, single-shot CARS spectra (100 up to 300 acquisitions) are recorded and stored in the laboratory computer. Then, the experimental data processing involves: background subtraction, CARS spectra smoothing, CARS spectra normalizing by a non-resonant CARS spectrum generated in argon. Temperature is determined by comparing spectral contours of experimental and theoretical CARS spectra. The latter is directly fitted to the experimental data by using a least square minimization routine. With this in mind to speed up process of the experimental data processing, these theoretical CARS spectra were calculated in 10-degree steps over the rotational and vibrational temperature range between 200 and 2000 K and stored in a library file.

Numerical modelling of the CARS spectra of different homonuclear molecules is based on theory and algorithms presented in detail [9–11,36,37] (see also papers quoted in Refs. [9–11,36,37] for further details). To create a theoretical spectra library a nonlinear third-order susceptibility is calculated. It is a complex function of quantum-mechanical parameters of hydrogen molecule and macroscopic parameters of gas media such as: pressure, gas temperature and population densities of vibrational and rotational levels, etc. The numerical simulation of the nonlinear third-order susceptibility includes consecutive calculation of Raman resonances, line-strength parameters, Raman cross-sections and linewidths. Besides, we correct this quantity to take into account Doppler broadening. The population densities of the vibrational and rotational levels are assumed to follow the Boltzmann law at the vibrational and rotational temperatures. This approximation is justified since we evaluate low rotational and vibrational states. Note also that the Raman cross-sections are strongly dependent on the rotational level number J and vibrational level number v, electronic spin statistical weight, polarizabilities and are calculated for O, Q and S transitions according to the relevant selection rules.

To define an apparatus function the following procedure has been used: first, we calculate convolution with the module square of the nonlinear third-order susceptibility with the pump laser lineshapes; then, results of this calculation are convolved with a detection system apparatus function. The apparatus function is deduced and parametered by comparison of theoretical and experimental H_2 CARS spectrum recorded at low pressures of 0.4−4 Torr and room temperature. It contains strong $Q_{01}(1)$ line at a small width (0.005−0.01 cm^{-1}) broadened by the Doppler effect [38,39]. It was well fitted by a Voigt profile and was characterized by a spectral width 3.0 cm^{-1} (FWHM). The largest contribution to the overall lineshape was given by the detection system apparatus function. Besides, this experimental spectrum is also used to determine dispersing grating law. To compare theoretical and experimental CARS spectra, the latter are transformed to the same scale of the theoretical spectra by using polynomial functions of the second order, describing dispersing grating law.

Finally, the theoretical spectra from the library are fitted to the experimental spectra to build temperature histograms and to calculate the average temperature and its standard deviation.

The validity of the second approach is due to the small Q-line spectral width compared with the distance between lines and does not depend on the rotational quantum number J under our experimental conditions. Therefore, the observable partial line superposition for the rotational lines with $J = 0$ and $J = 1$ is caused by the low spectral resolution of our apparatus. In this approach, for each selected spectral CARS line of Q-branch, computer code calculates the area from the fit of the spectral CARS line shapes with an automatic baseline correction. Since the Q-line shapes for the rotational number $J = 0$ and $J = 1$ partially overlap, multiple profile fitting is performed. Such multi-profile fitting is necessary to obtain the correct area from overlapping the Q-lines. The experimental CARS

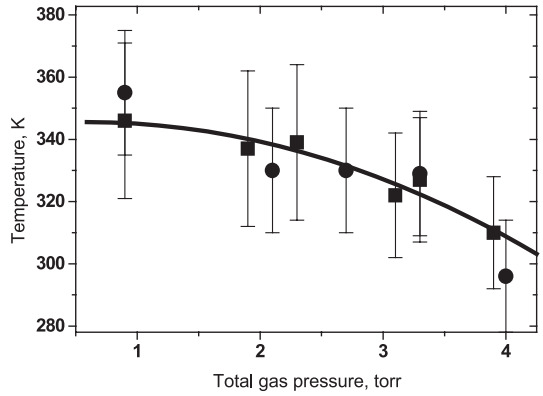

Fig. 3. Variation of the rotational temperature in the r.f. discharge plasma as function of the total pressure. The temperature surface of the grounded electrode is floating. Points indicate experimental data. Solid line is the result of experimental data fitting. Solid squares (■) denote values of the rotational temperature evaluated by processing CARS spectra data, as has been illustrated in Figure 2. Solid circles (•) indicate values of the rotational temperature deduced from rotational Q-line amplitudes.

spectra are smoothed and normalized by a non-resonant CARS spectrum generated in argon and averaged over laser shots. The square root of these quantities is proportional to population densities of the rotational levels at low rotational temperature $T_{rot} < 400$ K [23] and, thus, determines the rotational distribution. They were further normalized by the rotational degeneracy, nuclear spin degeneracy and Raman linestrength of each transition of the Q-branch [27]. In addition, we have determined the rotational temperature by using the Boltzmann plot technique.

4 Results and discussion

Capability of multiplex H_2 CARS technique is demonstrated in Figure 3.

The plot shows variation of the rotational temperature with the total pressure in the r.f. discharge plasma, determined by the different approaches. The CARS spectra were taken from the central part of the r.f. discharge plasma at a distance of 8 mm from the powered electrode surface. The solid circles indicate values of the rotational temperature deduced from the rotational line amplitudes. The solid squares denote values of the average temperature evaluated as a result of the CARS spectra processing, as illustrated in Figure 2. It is seen that the values obtained by the different approaches are in agreement within the experimental error. These values are close to room temperature and fall in the range between 300 and 360 K. Note that the obtained results regarding the values of temperature are quantitatively consistent with results reported in references [6,23,26]. Small differences between observed temperatures are a consequence of the high thermal gas conductivity of hydrogen molecules and of the small energy release power in the r.f. discharge plasma.

The observable spread in values of temperature is caused, first, by a small width of spectral lines of hydrogen molecule and fluctuations of radiation spectrum of pump lasers, and, second, by an instability of reproducibility of the r.f. discharge plasma parameters from experiment to experiment.

With increasing pressure the rotational temperature decreases (see Fig. 3). The temperature-pressure relationship is atypical of r.f. power mode operation, resulting in a poor quality discharge in a range of total pressure higher than 2.5 Torr. The fall-off in temperature is possibly caused by the limited amount of r.f. power available, which cannot support stable plasma at higher pressure. This observation is qualitatively consistent with the experimental results reported in reference [28].

It is common knowledge that to maintain high spatial resolution, at temperature CARS monitoring in combustion systems and discharges, it is preferably to use the BOXCARS arrangement [9–11]. Its application is mainly limited by poor signal-to-noise ratio as number density decreases and temperature increases. To improve multiplex H_2 CARS system detectability at temperature measurements, we used the collinear beam arrangement. However, it should be employed with care, since it results in a number of disadvantages [15,27,31]. Among them, as mentioned above, the size of the CARS probe volume is not well defined. Because of this, we also detected some CARS signals generated far from the local spot, i.e. from the gas volumes at different temperatures and number densities. If strong gradients are present along the beam axis, it can lead to erroneous temperature and number density measurements. It must be added that the fluctuations of the non-resonant signal created by the windows of the r.f. discharge reactor, by the remote resonance and electronic non-linearities of hydrogen and atmospheric nitrogen on way to the chamber, can also markedly affect the accuracy of the CARS measurements.

To be sure that the result of the temperature measurement is unaffected by the above-listed disadvantages arising from the use of the collinear beam arrangement, we have carried out a number of experiments with the purpose of comparing the rotational temperatures measured in both geometrical schemes of the pump laser beam mixing. Furthermore, these measurements were useful as calibration means for CARS technique. In these experiments the molecular hydrogen was heated to several hundreds Kelvin under equilibrium conditions, when the r.f. discharge plasma is off. The temperature measurements were performed at a distance of about 1 mm from the surface of the heated grounded electrode. Its temperature varied from 300 up to 650 K at a hydrogen pressure of 30 Torr. Under these conditions, an excellent signal-to-noise ratio for the BOXCARS arrangement was reached. Figure 4 gives the rotational temperature comparison. Here, solid squares and triangles indicate results of the temperature measurements as a function of electrode temperature, in both the collinear beam and the planar BOXCARS arrangements, respectively. As it is evident from Figure 4, these values are in good agreement within the

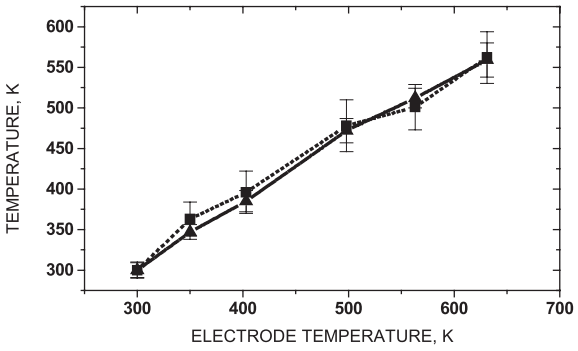

Fig. 4. Variation of the rotational temperature as function of the grounded electrode temperature. Solid squares (■) and triangles (▲) denote values of the rotational temperatures measured in both the collinear and planar BOXCARS arrangements, respectively, at hydrogen pressure 30 Torr.

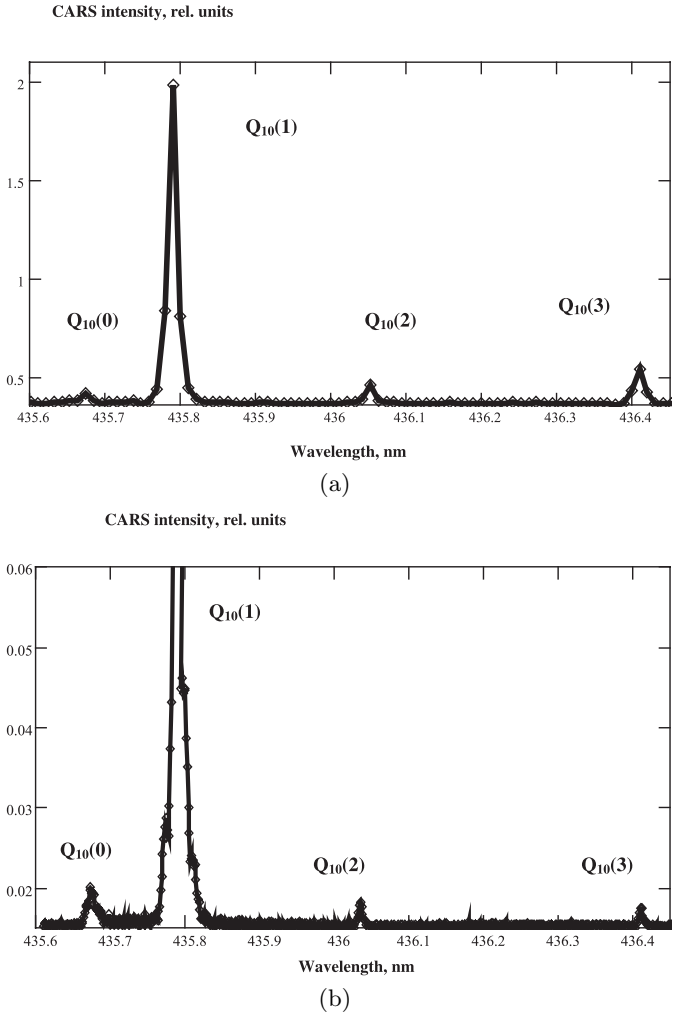

Fig. 5. CARS spectrum of the Q-branch of the vibrational transition from $v = 0$ to $v = 1$ of the hydrogen molecule recorded by using narrow-band CARS spectroscopy at total gas pressure 2.0 Torr. Points are experimental data. Solid lines are result of experimental data fitting. (a) CARS spectrum of heated hydrogen up to 490 K under equilibrium conditions (i.e. without RF discharge). (b) CARS spectrum of hydrogen in the r.f. discharge plasma at the rotational temperature about 330 K. This plot is presented on an enlarged scale.

experimental error with temperature measurements. The interelectrode distance, small compared to the size of the electrodes, causes homogeneous spatial distribution of the gas temperature and number density over the length of the CARS probe volume in both the beam arrangements. Quantitative agreement between values of the temperatures proves the suitability of the collinear beam arrangement for the r.f. discharge geometry used. It should be noted that the rotational temperature coincides with that of the grounded electrode in a range of temperatures from 300 to 450 K, thus testifying the reliability of the used technique. The lower limit of detection for hydrogen in the r.f. discharge plasma, i.e. when it is still possible to evaluate the rotational temperature from the CARS spectrum with the use of the collinear beam arrangement, is approximately around 0.4−0.6 Torr.

The coincidence of the rotational temperature with the translational one is a key question from the standpoint of the gas temperature determination in H_2 r.f. discharge plasma. It was recognized [31–34] that, in presence of a Boltzmann rotational distribution, the rotational temperature deduced by measuring the ratio of population densities for rotational levels with $J = 0$ and $J = 1$ was in good agreement with the translational ones.

Figures 5a and 5b show typical recorded CARS spectra by using the method of narrow-band CARS spectroscopy, which were taken from an equilibrium heated gas and in the r.f. discharge plasma, respectively. Figure 6 reports the corresponding rotational distribution CARS spectra. The points indicate the natural logarithm of the population density N_J normalized with the statistical weight $J(J+1)$ times the nuclear spin σ_J. In contrast to results described in references [32,33], no deviations of the rotational distribution from the Boltzmann law is observed for low rotational levels with $J = 0$−3. As can be seen from Figure 6, the experimental population densities of the hydrogen molecules with $J = 0$−3 can be represented, to a good approximation, according to Boltzmann law. The obtained result is consistent with that reported [7,31,34]. The observed distribution behaviour implies that the values of the measured rotational temperatures presented in references [31,34], as well as our findings (see Fig. 3), are higher than those reported in references [32,33]. The enhancement of temperature and pressure tends to increase rate constants of the rotational-translational relaxation [2,3] and destroys deviation of the rotational distribution from Boltzmann law, occurring within the limits of specific spin modifications of hydrogen molecule (para-hydrogen and ortho-hydrogen) [32,33].

Table 1 presents the temperatures, which were derived from the slope of a least–squares fit to a Boltzmann distribution (solid lines). It was found that the effective rotational temperatures T_{rot}, corresponding to measured rotational distribution, are in a good agreement in the limits of standard deviation, with temperature values, corresponding to a pair of levels $J = 0$, 2 (para-hydrogen) T_{02} and

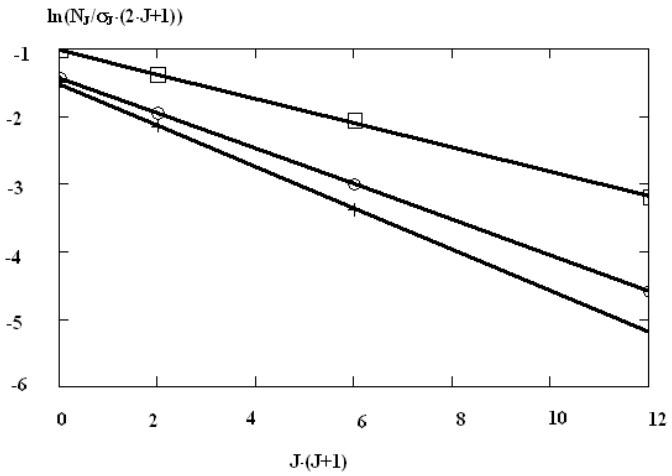

Fig. 6. The rotational distribution functions deduced from the Q-line amplitudes at the total pressure 2.0 Torr. Solid lines are a least-squares fit to Boltzmann's plot; (+) rotational distribution function at room temperature, (∘) rotational distribution function in the r.f. discharge at rotational temperature of 330 K, (□) rotational distribution function of heated hydrogen up to 490 K at equilibrium condition.

Table 1. Comparison among temperatures.

T_{rot}, K	T_{13}, K	T_{02}, K	T_{01}, K	T_{term}, K
300 ± 20	290 ± 20	280 ± 20	290 ± 20	300 ± 20
480 ± 20	480 ± 20	490 ± 20	490 ± 20	490 ± 20
330 ± 20	330 ± 20	340 ± 20	330 ± 20	—

a pair of levels with $J = 1$, 3 (ortho-hydrogen) T_{13}, as well as, the rotational temperature T_{01} deduced by measuring population density ratio for rotational levels with $J = 0$ and $J = 1$. Note that the measured temperatures by CARS spectroscopy at equilibrium conditions and by thermocouple T_{term} are also in good agreement. Thus, we can conclude, that the measured rotational temperature under our experimental conditions can be considered to be equal to the gas temperature in the investigated range of the total pressure. Therefore, the rotational temperature can be taken equal to the gas one.

To analyse the experimental multiplex CARS spectra and to evaluate the rotational temperature, numerical modelling of multiplex CARS spectra were carried out in a range of wave numbers, which correspond to the spectral positions of the rotational structure of the Q-branch of the vibrational-rotational transitions $v = 0 \rightarrow v = 1$ and $v = 1 \rightarrow v = 2$ of the hydrogen molecule.

Figures 7a and 7b show theoretical multiplex CARS spectra of the hydrogen molecule obtained as a result of the numerical modelling versus the rotational temperature under equilibrium conditions. Note that for reasons of convenience, when comparing calculated and experimental spectra, the pixel position of the detector is plotted. As can be drawn from Figure 7a, simple structure of the Q-branch with the partially resolved rotational structure of the vibrational-rotational transition $v = 0 \rightarrow v = 1$ is observed due to low values of the rotational temperature. It mainly consists of the Q-lines, corresponding to rotational numbers $J = 0{-}3$. Here, $Q_{01}(0-3)$ denote the Raman transitions from $v = 0$, $J \rightarrow v = 1$, J, which are assigned to the fundamental band, the so-called "cold band". For higher temperatures $T > 2000$ K (see Fig. 7b), as population densities of rotational levels with $J = 5{-}7$ increase, it is also possible to observe strong Q-lines, corresponding to $Q_{01}(5-7)$ transitions. Population density on the vibrational level $v = 1$ is no longer small so that besides the Q-lines of the fundamental band, $Q_{12}(1)$ transition ($v = 1 \rightarrow v = 2$) of weak intensity, the so-called "hot band", appears.

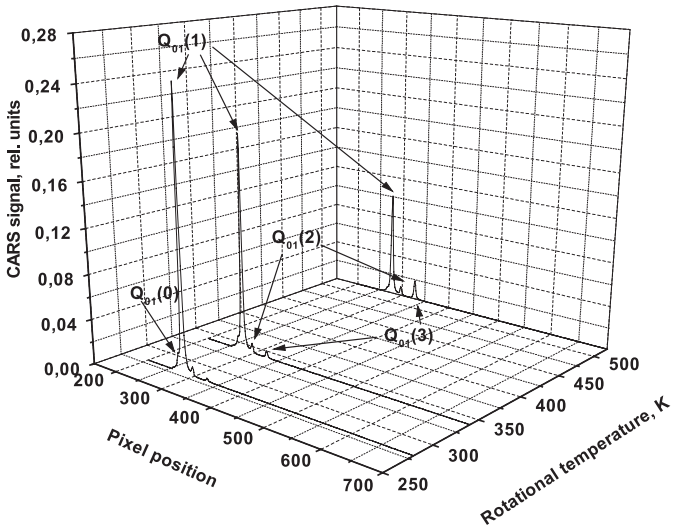

(a)

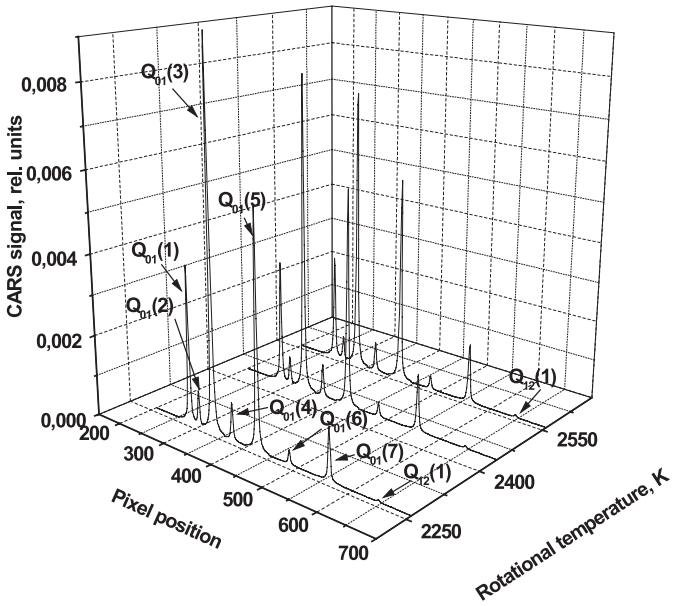

(b)

Fig. 7. Calculated multiplex H_2 CARS spectra at the equilibrium conditions and at gas pressure 2.0 Torr for the rotational temperatures: (a) $T_{rot} = 280$, 340 and 520 K; (b) $T_{rot} = 2260$, 2440 and 2560 K. Q-lines are labeled by their J-numbers.

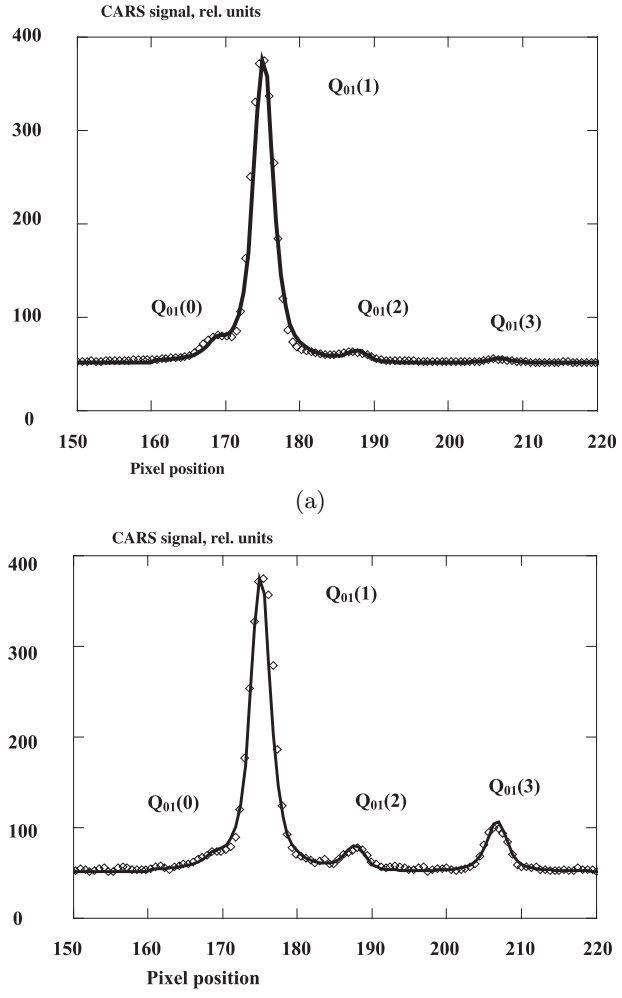

Fig. 8. (a) Room temperature CARS spectrum of hydrogen. (b) Single shot CARS spectrum of hydrogen at the equilibrium conditions, open diamonds, and theoretical fit, solid line. The best fit theoretical spectrum corresponds to a temperature of 490 K. The gas pressure is equal to 30 Torr.

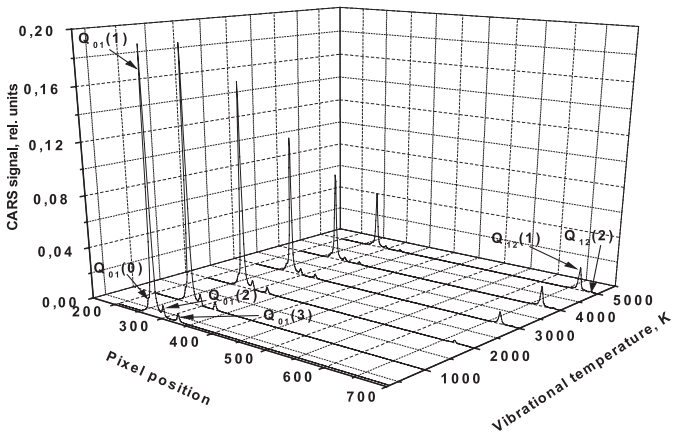

Fig. 9. Calculated multiplex H_2 CARS spectra as function of the vibrational temperature at the nonequilibrium conditions and at the total pressure 2.0 Torr. The rotational temperature is equal to 340 K. Q-lines are labeled by their J-numbers.

Figure 8 illustrates, as an example, theoretical multiplex CARS spectra fitting to experimental ones under equilibrium conditions, when discharge is off. The points indicate experimental data obtained by using BOXCARS arrangement, in single laser shot, normalized to the nonresonance CARS signal generated from argon. The solid line refers to results of the numerical simulation of CARS spectrum. As consistency check of the room temperature spectrum, Figure 8a demonstrates a correlation of the typically measured and calculated CARS spectra at room temperature. Figure 8b also presents a comparison between experimental H_2 CARS spectrum, which was taken from the molecular hydrogen heated at 510 K at the equilibrium conditions, and calculated ones. The best fitting between calculated and experimental CARS spectra is reached for the rotational temperature, which is equal to 490 K. The calculated and measured CARS spectra under equilibrium conditions are in good agreement with corresponding spectra reported in literature [9,25,28,36].

Figure 9 shows the calculated multiplex CARS spectra as function of the vibrational temperature in a range from 340 to 5000 K for a rotational temperature of 340 K. The Q-lines with rotational numbers $J = 1$ and 2 of the "hot band" occur at values of the vibrational temperature higher than 1600−2000 K. Vibrational-rotational transition, corresponding to the "hot band", has poorly expressed rotational structure due to low value of the rotational temperature. For the experimental CARS spectra recorded in the r.f. discharge plasma, no strong lines attributable to excited vibrational states were observed, apparently because signal intensities did not exceed the noise level at low values of vibrational temperatures. In fact, calculated ratios $Q_{21}(1)$ over $Q_{10}(1)$ are equal to 0.01 at a vibrational temperature of 2000 K. It was approximately coincident with typical values of ratio of noise to amplitude of CARS signal $Q_{10}(1)$ recorded in experiment. This experimental observation points out that the sensitivity of our multiplex H_2 CARS system is not sufficient for detection of the Q-lines relative to the vibrational-rotational transition $v = 1 \rightarrow v = 2$ at both low pressures and vibrational temperatures. The obtained results are consistent with those reported in reference [26]. Besides, the numerical modelling of vibrational kinetics of molecular hydrogen in both low pressure dc glow [40] and radio frequency [41] discharges also confirms that the value of vibrational temperature does not exceed 2000 K.

Numerical simulation shows that the variation of the vibrational temperature from 340 to 2000 K does not essentially affect the result of the rotational temperature evaluation. Figures 10a and 10b illustrate a comparison between calculated and experimental CARS spectra taken from the r.f. discharge plasma by using the collinear beam arrangement at total gas pressure 2.0 Torr. Figure 10a indicates that the amplitudes of CARS signals appropriate to vibrational-rotational transitions $Q_{01}(0)$, $Q_{01}(2)$ and $Q_{01}(3)$ are much lower than the amplitude $Q_{01}(1)$

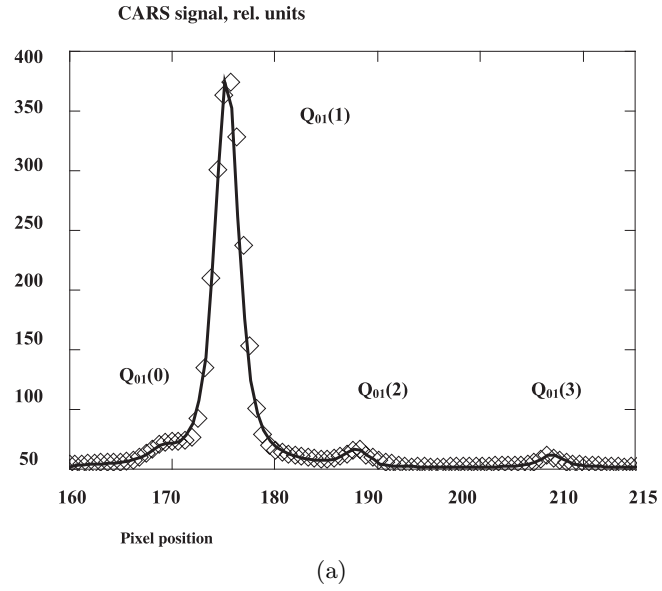

Fig. 10. (a) Single shot CARS spectrum of hydrogen in the r.f. discharge plasma, open diamonds, and theoretical fit, solid line. The best fit theoretical spectrum corresponds to a temperature of 340 K. The total pressure is equal to 2.0 Torr. The plot (b) is presented on an enlarged scale (see text).

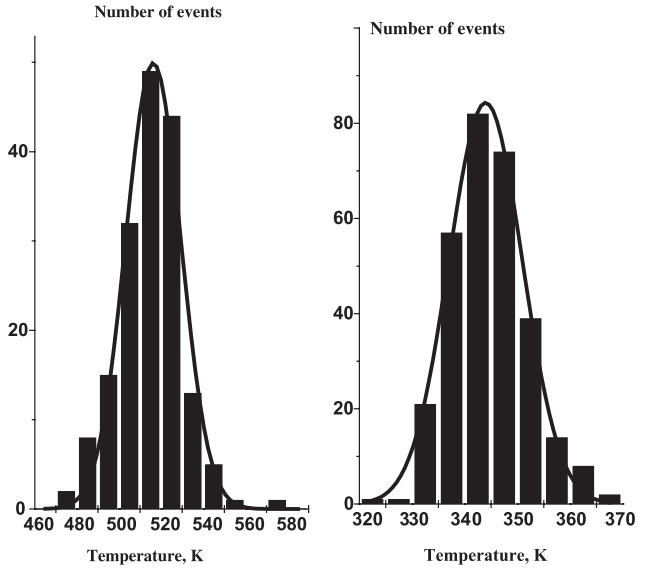

Fig. 11. (a) Histogram of the rotational temperature values deduced from 170 single-shot CARS spectra taken from the molecular hydrogen heated to 510 K at pressure 30 Torr and at the equilibrium conditions. (b) Histogram of the rotational temperature values deduced from 300 single-shot CARS spectra obtained in the r.f. discharge plasma at the total pressure 2.0 Torr. The solid line is the normal distribution function fit to the data.

owing to the low value of the rotational temperature. As a consequence, this representation does not adequately describe the result of fitting (solid line) for these transitions. To avoid this disadvantage, Figure 10b demonstrates results of fitting for vibrational-rotational transitions $Q_{01}(0)$, $Q_{01}(2)$ and $Q_{01}(3)$ on an enlarged scale. As indicated in Figures 10a and 10b, the best agreement between them is attained when the rotational temperature is 340 K. During experimental data processing, it was observed that values of temperature, recovered from single shot CARS spectrum, exhibit fluctuations. For this reason, we recorded up to 300 single-shot CARS spectra at a given position of the probe CARS volume inside the r.f. discharge reactor chamber to determine the average temperature and its standard deviation. Figures 11a and 11b present typical rotational temperature histograms obtained under thermally excited hydrogen flow and under hydrogen r.f. discharge plasma, respectively. The solid line denotes the probability distribution function. In both cases, it is characterized by a Gaussian distribution having the relative standard deviation of about 5−7%. Therefore we believe that no instabilities of the r.f. discharge plasma contribute significantly to the relative standard deviation during temperature measurement. Temperature fluctuations are directly connected to instability of the spectral shape and amplitude of the CARS spectrum, which change shot by shot. According to results reported by reference [44], instability in CARS spectra is due to the small width of spectral lines of the hydrogen molecule and fluctuations of radiation spectrum of broadband dye laser. It is necessary also to add fluctuations of frequency, phase and distribution of energy in a beam of Nd–YAG laser, detector noise and experimental equipment mechanical vibrations [21,43]. The obtained standard deviation of 7% is appreciably lower than those previously achieved by H_2 CARS thermometry [42] and two-wavelength CARS thermometry based on S-branch rotational transitions in the hydrogen molecule [43], which are typically 15% and 11%, respectively. But, it is comparable with results reported in reference [28] and larger than those achieved by fast two-wavelength CARS

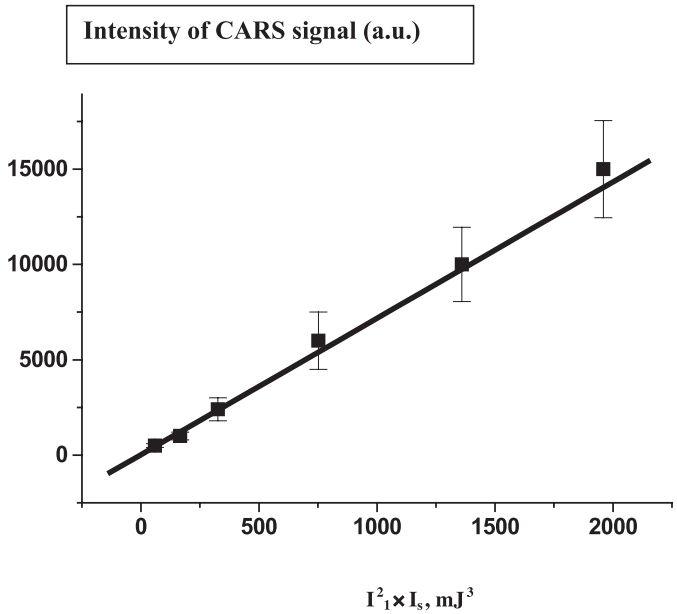

Fig. 12. Control of the saturation behavior as a function of the product of the square of the pump intensity I_1 of the Nd–YAG laser and of the pump intensity I_s of the broadband dye laser at gas pressure 2 Torr.

thermometry of nitrogen discharges [21], in conventional scanning narrow-band or single shot N_2 CARS spectroscopy [12–16,18–20,22–24,26,27,30–34,44] (around 3−5%) because of the high spectral density of the transitions in the nitrogen molecule. However, in spite of the large error, the presented multiplex H_2 CARS thermometry reduces the time needed to measure the gas temperature down to several tens of seconds, as opposite to the method of scanning narrow-band CARS spectroscopy, where acquisition of a scanned CARS spectrum requires several ten of minutes. The amplitude, spectral shape and positions of lines in the CARS spectrum generated in intense pump laser fields at a low density can appreciably be distorted. This makes an analysis of an observable CARS spectrum more difficult and results in errors of temperature and concentration measurements. According to results reported by [45,46], at a low density, in the intense pump laser fields, shift of molecule energy levels due to dynamic Stark's effect is observed. A negative displacement of the Raman resonance positions results. Besides, the strong laser fields can cause significant redistribution of populations on energy levels. The saturation behaviour in CARS spectrum results. As it was shown in references [28, 46], under our experimental conditions, the saturation behavior is dominated by velocity changing collisions which effectively couple all velocity groups within the Doppler broadened line. To check up presence of the saturation behaviour and dynamic Stark's effect in the CARS spectra the study of dependence of the $Q_{01}(1)$ line intensity on the product of the squared Nd–YAG laser radiation intensity by the intensity of the broadband dye laser $I_s \times I_1^2$ was carried out. Figure 12 presents results of this measurement. The points, solid square in Figure 12, indicate values of the CARS intensities versus $I_s \times I_1^2$ recorded at room temperature in the planar BOXCARS arrangement. Each point on the graph corresponds to the average of 300 laser shots. This dependence shows good linear relations, as predicted by CARS theory [9–11]. Thus, it is possible to assume, that the saturation behaviour and dynamic Stark's effect in the CARS spectra are insignificant and slightly influence results of the gas temperature measurement.

5 Conclusions

In the present study, we have shown the capability of multiplex CARS spectroscopy for thermometry in the radio-frequency capacitive discharge plasma in molecular hydrogen at low gas temperatures (300−400 K), pressure in the range 0.4−4 Torr and power 100 W. Population densities of rotational levels with $J = 0$−3 in the ground electronic state of hydrogen molecules and measurements of the rotational temperature by multiplex H_2 CARS spectroscopy in the r.f. capacitive discharge plasma have been reported. Computational codes have been developed to determine the rotational and vibrational temperature and to analyze H_2 CARS spectra under thermal and discharge conditions. The experimental population densities of the hydrogen molecule can be reproduced, to a good approximation, by Boltzmann laws. The values of the rotational temperature deduced from the measured rotational distribution function agree well within the experimental uncertainty with those determined from the ratio of populations in rotational states $J = 1$ and $J = 3$ (ortho-hydrogen), $J = 0$ and $J = 2$ (para-hydrogen), as well as, from the ratio of populations in rotational states $J = 0$ and $J = 1$. Under our experimental conditions, the measured rotational temperature can be considered to be equal to the gas ones in the investigated range of the total pressure. The developed multiplex H_2 CARS apparatus and computer codes reduce the time needed to measure the rotational temperature down to several tens of seconds, as opposite to the method of scanning narrow-band CARS spectroscopy, where acquisition of a scanned CARS spectrum requires several tens of minutes. The lower limit of detection for hydrogen in the r.f. discharge plasma was around 0.4−0.6 Torr with our apparatus. Temperatures were obtained with an accuracy given by a standard deviation of 7%. The experimental CARS spectra recorded in the r.f. capacitive discharge plasma show no Q-lines of the vibrational-rotational transition $v = 1$–$v = 2$. A number of improvements in the apparatus are planned which should markedly improve the detection capability.

We thank Dr. K.A. Vereschagin for suggestions in this work and Prof. H.F. Dobele for reading the manuscript. This work was supported by ASI (I/R/038/01) and (I/R/055/02).

References

1. *Plasma Technology: Fundamentals and Applications*, edited by M. Capitelli, C. Gorse (Plenum press, New York and London, 1992)

2. Y.P. Raizer, M.N. Shnaider, N.A. Yatsenko, *Radio-Frequency Capacitive Discharges: Physics. Experimental technique. Applications* (Fiz. Publ. Comp., Moscow, 1995, *in Russian*)
3. *Nonequilibrium Vibrational Kinetics*, edited by M. Capitelli, Topics in Current Physics series (Springer-Verlag, Berlin, 1986), Vol. 39
4. *Plasma diagnostics*, edited by W. Lochte-Holtgreven (American Elsevier, New-York, 1968)
5. W. Demtroder, *Laser spectroscopy, Basic concepts and instrumentation* (Springer-Verlag, Berlin, Heidelberg, New York, 1982)
6. T. Gans, V. Schulz-von der Gathen, H.F. Dobele, Plasma Sources Sci. Technol. **10**, 17 (2001)
7. T. Mosbach, H.M. Katsch, H.F. Dobele, Phys. Rev. Lett. **85**, 3420 (2000)
8. B.P. Lavrov, A.A. Sobol'ev, M.V. Tyutchev, J. Appl. Spectrosc. **32**(4), 316 (1980)
9. J.W. Nibler, G.V. Knighten, in *Raman Spectroscopy of Gases and Liquids*, edited by A. Weber (Springer-Verlag Berlin, Heidelberg, New York, 1979), pp. 253-299
10. S.A. Druet, J.-P.E. Taran, Progr. Quant. Electron. **7**(1), 1 (1981)
11. R.J. Hall, A.C. Eckbreth, Laser Appl. **5**, 214 (1984)
12. W.M. Shaub, J.W. Nibler, A.B. Harvey, J. Chem. Phys. **67**(5), 1883 (1977)
13. V.V. Smirnov, V.I. Fabelinskii, JETP Lett. **28**, 424 (1978)
14. S.I. Valyanskii, K.A Vereschagin, V. Vernke, A.Yu. Volkov, P.P. Pashinin, V.V. Smirnov, V.I. Fabelinskii, P.L. Chapovskii, Sov. J. Quant. Electron. **14**, 1226 (1984)
15. B. Massabieaux, G. Gousset, M. Lefebvre, M. Pealat, J. Phys. France **48**, 1939 (1987)
16. A.V. Bodronosov, K.A. Vereschagin, V.A. Gorshkov, K.V. Khodataev, V.A. Shakhatov, Tech. Phys. **39**(1), 25 (1994)
17. A.V. Bodronosov, K.A. Vereschagin, V.A. Gorshkov, V.V. Smirnov, K.V. Khodataev, V.A. Shakhatov, Quant. Electron. **24**(9), 832 (1994)
18. O.A. Gordeev, V.A. Shakhatov, Tech. Phys. **40**(7), 656 (1995)
19. V.A. Shakhatov, Determination of the rate constants for VV exchange in a nitrogen glow discharge by CARS spectroscopy, *European Conference Abstracts: ESCAMPIG XIIIth*, Poprad (Slovakia), 1996, Vol. 20E, Part B, p. 449
20. A.V. Bodronosov, K.A. Vereschagin, O.A. Gordeev, V.V. Smirnov, V.A. Shakhatov, High Temp. **34**(5), 656 (1996)
21. A.V. Bodronosov, K.A. Vereschagin, V.A. Gorshkov, V.V. Smirnov, K.V. Khodataev, V.A. Shakhatov, Quant. Electron. **24**(9), 832 (1994)
22. K.A. Vereschagin, V.V. Smirnov, V.A. Shakhatov, Tech. Phys. **42**(5), 487 (1997)
23. J.W. Nibler, J.R. McDonald, A.B. Harvey, Opt. Commun. **18**(3), 371 (1976)
24. J.A. Shirley, R.J. Hall, J. Chem. Phys. **67**(6), 2419 (1977)
25. V. Kornas, V. Shulz-von der Gathen, T. Bornemann, H.F. Dobele, G. Prosz, Plasma Chem. Plasma Process. **11**(2), 171 (1991)
26. S.O. Hay, W.C. Roman, M.B. Colket III, J. Mater. Res. **5**(11), 2387 (1990)
27. Chen Kuei-Hsien, Chuang Mei-Chen, C. Murray Penney, W.F. Banholzer, J. Appl. Phys. **71**(3), 1485 (1992)
28. C.F. Kaminski, P. Evart, Appl. Phys. B **64**, 103 (1997)
29. K.E. Bertagnolli, R.P. Lucht, Temperature profile measurements in stagnation-flow diamond-forming flames using hydrogen CARS spectroscopy, *Proc. 26th Int. Symp. On Combust.,* Pittsburgh, Pa., 1997, pp. 1825-1833
30. M. Ganz, N. Dorval, M. Lefebvre, M. Pealat, F. Loumagne, F. Laglais, J. Electrochemi. Soc. **143**(5), 1654 (1996)
31. M. Pealat, J.-P.E. Taran, M. Bacal, F. Hilion, J. Chem. Phys. **82**(11), 4943 (1985)
32. B.U. Asanov, V.N. Ochkin, S.Yu. Savinov, N.N. Sobolev, S.N. Tskhai, Sov. Phys. - Lebedev Inst. Rep. (USA), No. **9**, 1986, pp. 40-44
33. V.N. Ochkin, S.Yu. Savinov, N.N. Sobolev, S.N. Tskhai, Sov. Phys. - Tech. Phys. (USA) **33**(7), 763 (1988)
34. M. Lefebvre, M. Pealat, J.-P.E. Taran, Pure Appl. Chem. **64**(5), 685 (1992)
35. S.A. Astashkevich, M.V. Kalachev, B.P. Lavrov, V.L. Ovtchinnikov, Opt. Spectrosc. **87**(2), 203 (1999)
36. J.C. Luthe, E.J. Beiting, F.Y. Yueh, Comput. Phys. Commun. **42**, 73 (1986)
37. P. Huber-Walchli, J.W. Nibler, J. Chem. Phys. **76**(1), 273 (1982)
38. R.A.J. Keijser, J.R. Lombardi, K.D. Van Den Hout, B.C. Sanctuary, H.F.P. Knaap, Physica **76**, 585 (1974)
39. A. Rahn, R.L. Farrow, Phys. Rev. A **43**(11), 6075 (1991)
40. C. Gorse, M. Capitelli, A. Ricard, J. Chem. Phys. **82**(4), 1900 (1985)
41. S. Longo, A. Milella, Chem. Phys. **274**, 219 (2001)
42. W. Strieker, M. Woyde, R. Luckerath, V. Bergmann, Ber. Bunsenges. Phys. Chem. **97**(12), 1608 (1993)
43. K.A. Vereshchagin, W. Clauss, D.N. Kozlov, D.Yu. Panasenko, V.V. Smirnov, O.M. Stel'makh, V.I. Fabelinskii, V.A. Shakhatov, Quant. Electron. **27**(11), 1019 (1997)
44. S. Prucker, W. Meier, W. Stricker, Rev. Sci. Instrum. **65**(9), 2908 (1994)
45. M. Pealat, M. Lefebvre, J.-P.E. Taran, P.L. Kelley, Phys. Rev. A **38**(4), 1948 (1988)
46. R.P. Lucht, R.L. Farrow, JOSA B **5**(6), 1243 (1988)